EUROPEAN ORGANIZATION FOR NUCLEAR RESEARCH (CERN)

CERN-PH-EP-2014-203
LHCb-PAPER-2014-044
January 29, 2016

Measurements of *CP* violation in the three-body phase space of charmless $B^{\pm}$ decays (ADDITIONAL INFORMATION)

The LHCb collaboration

Abstract

This document presents figures of the projections into the two-body invariant masses of the spectra of $B^{\pm} \to K^{\pm}\pi^{+}\pi^{-}$, $B^{\pm} \to K^{\pm}K^{+}K^{-}$, $B^{\pm} \to \pi^{\pm}K^{+}K^{-}$ and $B^{\pm} \to \pi^{\pm}\pi^{+}\pi^{-}$ decays. The figures show additional information related to the *CP* asymmetry in phase space, for section VII of the article Physical Review D 90, 112004 (2014).

© CERN on behalf of the LHCb collaboration, license CC-BY-4.0.

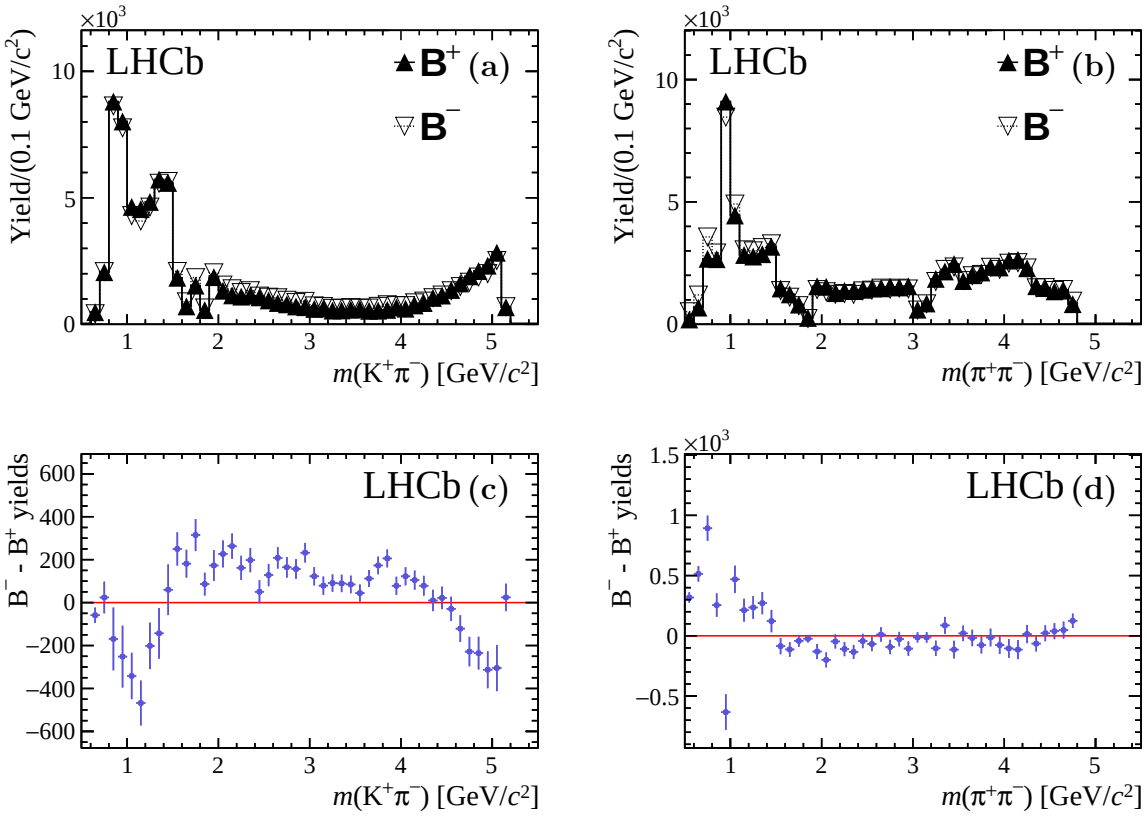

Figure 1: Projections in bins of the $m(K^{\pm}\pi^{\mp})$ and $m(\pi^{+}\pi^{-})$ variables of (a), (b) the number of B^{-} and B^{+} signal events and (c), (d) their difference for the $B^{\pm} \to K^{\pm}\pi^{+}\pi^{-}$ decays. The yields are acceptance-corrected and background-subtracted. A guide line for zero (horizontal red line) is included in plots (c) and (d).

1 Two-body invariant mass projections

In Ref. [1] the $A_{\rm raw}^{N}$ distributions in the Dalitz plots reveal rich structures, which are more evident in the two-body invariant-mass projection plots. Figures 1, 2, 3 and 4 show the whole spectrum of the two-body invariant-mass projections for the $B^{\pm} \to K^{\pm}\pi^{+}\pi^{-}$, $B^{\pm} \to K^{\pm}K^{+}K^{-}$, $B^{\pm} \to \pi^{\pm}\pi^{+}\pi^{-}$ and $B^{\pm} \to \pi^{\pm}K^{+}K^{-}$ decays, respectively.

References

[1] LHCb collaboration, R. Aaij *et al.*, *Measurements of CP violation in the three-body phase space of charmless $B^{\pm}$ decays*, Phys. Rev. **D90** (2014) 112004, arXiv:1408.5373.

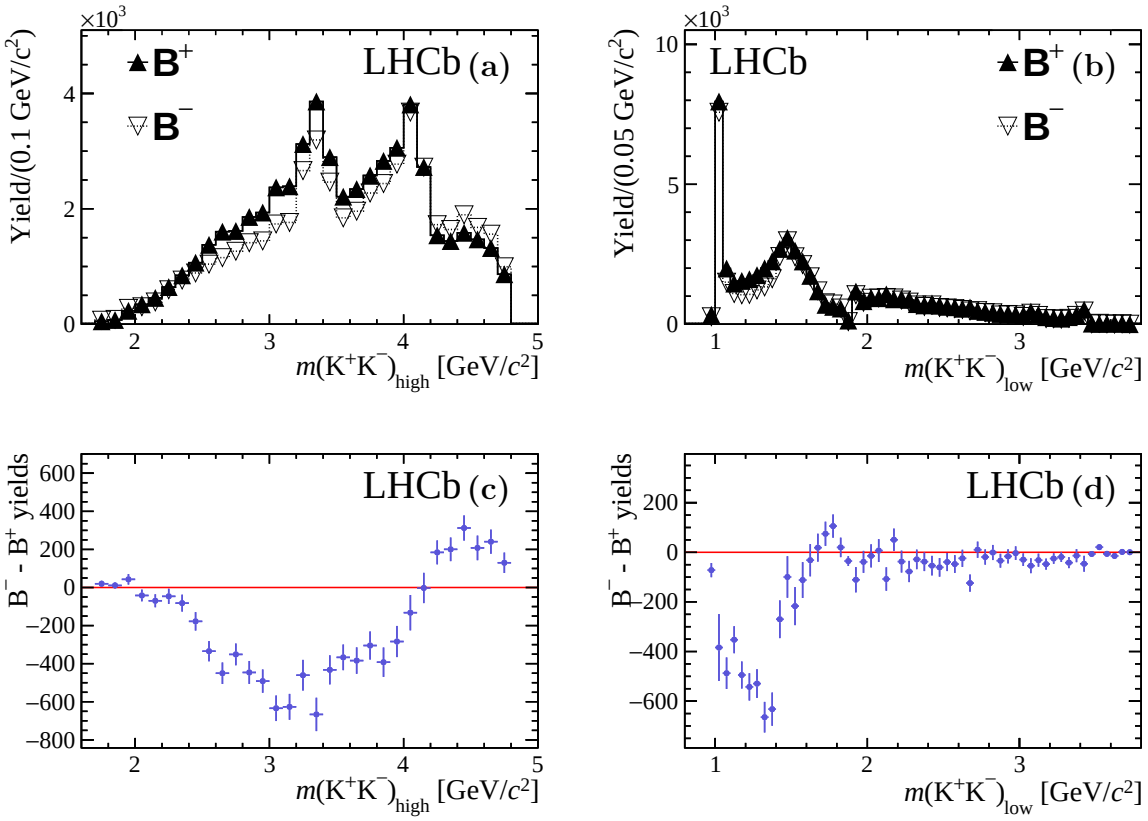

Figure 2: Projections in bins of the $m(K^+K^-)_{\rm high}$ and $m(K^+K^-)_{\rm low}$ variables of (a), (b) the number of B^- and B^+ signal events and (c), (d) their difference for the $B^\pm \to K^\pm K^+ K^-$ decays. The yields are acceptance-corrected and background-subtracted. A guide line for zero (horizontal red line) is included in plots (c) and (d).

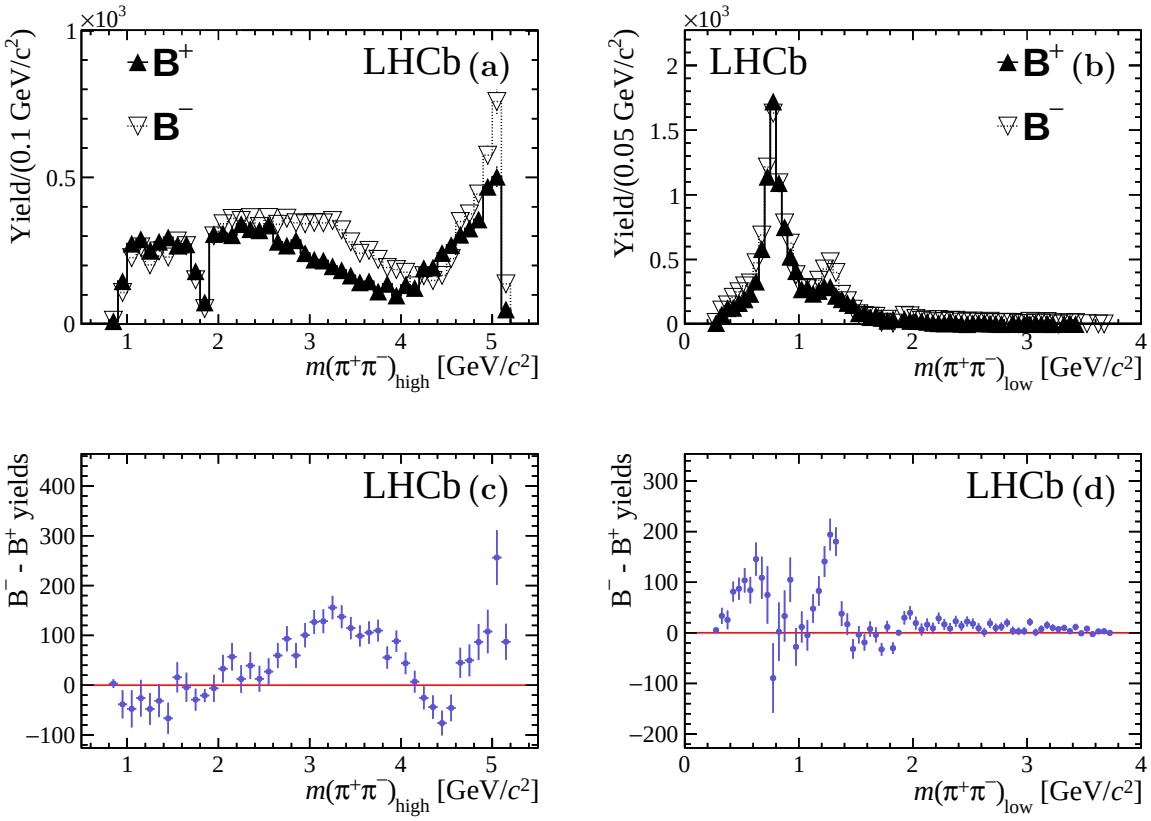

Figure 3: Projections in bins of the $m(\pi^+\pi^-)_{\rm high}$ and $m(\pi^+\pi^-)_{\rm low}$ variables of (a), (b) the number of B^- and B^+ signal events and (c), (d) their difference for the $B^\pm \to \pi^\pm\pi^+\pi^-$ decays. The yields are acceptance-corrected and background-subtracted. A guide line for zero (horizontal red line) is included in plots (c) and (d).

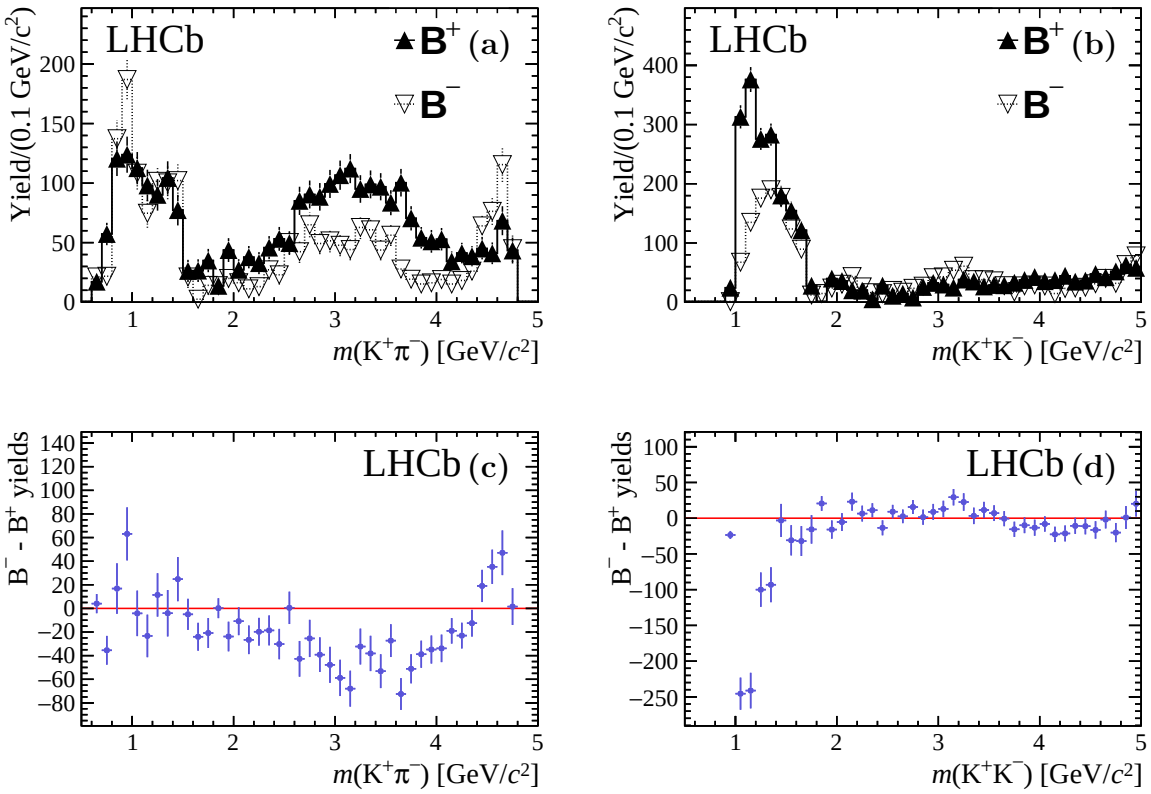

Figure 4: Projections in bins of the $m(K^{\pm}\pi^{\mp})$ and $m(K^+K^-)$ variables of (a), (b) the number of B^- and B^+ signal events and (c), (d) their difference for the $B^{\pm} \to \pi^{\pm}K^+K^-$ decays. The yields are acceptance-corrected and background-subtracted. A guide line for zero (horizontal red line) is included in plots (c) and (d).